

1 The 2018 version of the Global Earthquake 2 Model: Hazard component

3 **M. Pagani,^{a)} J. Garcia-Pelaez,^{a)} R. Gee,^{a)} K. Johnson,^{a)} V. Silva,^{b)} M. Simionato,^{c)} R.
4 **Styron,^{a)} D. Viganò,^{c)} L. Danciu,^{d)} D. Monelli,^{e)} V. Poggi,^{f)} and G. Weatherill^{g)}** **

5 In December 2018, at the conclusion of its second implementation phase, the Global
6 Earthquake Model (GEM) Foundation released its first version of a map outlining
7 the spatial distribution of seismic hazard at a global scale. The map is the result of
8 an extensive, joint effort combining the results obtained from a collection of prob-
9 abilistic seismic hazard models, called the GEM mosaic. Overall, the map and the
10 underlying database of models provide the most up-to-date view of the earthquake
11 threat globally. In addition, using the mosaic, a synopsis of the current state-of-
12 practice in modeling probabilistic seismic hazard at national and regional scales can
13 be created. The process adopted for the compilation of the mosaic adhered to the
14 maximum extent possible to GEM's principles of collaboration, inclusiveness, trans-
15 parency and reproducibility. For a given area, priority was given to seismic hazard
16 models either developed by well-recognized national agencies or by large collabo-
17 rative projects involving local scientists. The presented version of the GEM mosaic
18 contains 30 probabilistic seismic hazard models, 14 of which represent national or
19 sub-national models. The remainder are regional-scale models built by GEM itself
20 using open tools and methodologies. 

21 INTRODUCTION

22 Seismic hazard maps depict the geographic distribution of shaking intensity with a given an-
23 nual frequency (or probability) of exceedance. An alternative, although less common way to
24 portray the geographic distribution seismic hazard is the annual frequency (or probability) of
25 exceedance of a fixed ground motion level of an intensity measure type (e.g. peak ground

^{a)}Hazard Team, Global Earthquake Model, Pavia, Italy

^{b)}Risk Team, Global Earthquake Model, Pavia, Italy

^{c)}IT Team, Global Earthquake Model, Pavia, Italy

^{d)}Swiss Seismological Service, ETH, Zurich, Switzerland

^{e)}Tokyo Millennium, Zurich, Switzerland

^{f)}Centro Ricerche Sismologiche, OGS, Trieste, Italy

^{g)}GFZ German Research Centre for Geosciences, Potsdam, Germany

26 acceleration).

27 Hazard analyses are commonly classified based on the extent of the area covered by the
28 analysis. Typical scales of investigation include site-specific studies, seismic microzonations,
29 national, regional, and global hazard analyses. Very often, hazard maps are built at a national
30 scale, as this information forms the basis for defining building design actions. These large-
31 scale investigations, as opposed to the ones performed at urban and site scales, usually do not
32 incorporate site conditions, and instead provide hazard on “rock” (or reference site condition 
33 Global seismic hazard maps, such as the map presented here, inform specialists and common
34 people about the most seismically dangerous regions of the world 

35 Two approaches are available for constructing a global seismic hazard model and the sub-
36 sequent calculation of hazard. The first one involves subdividing inland territories into a num-
37 ber of areas and constructing independent hazard models for each of them. This approach was
38 used to construct the well-known Global Seismic Hazard Assessment Program (GSHAP) model
39 (Giardini et al., 1999), in which ten principal regional models were combined with additional
40 models covering specific areas, for example the PILOTO project for the Northern Andes (Di-
41 maté et al., 1999) or the CAUCAS project in the Caucasus region. The second approach tackles
42 the problem more radically by building a single seismic hazard model using fewer, but more
43 homogenous, methods and a data sets with global coverage (e.g. a global earthquake catalog,
44 a global database of active faults). This approach was used, for example, by Weatherill and
45 Pagani (2014) to explore the feasibility of a uniform approach to global hazard modeling and
46 by Ordaz et al. (2014) to support the risk calculation within the 2013 version of the Global
47 Assessment Report on Disaster Risk Reduction (GAR).

48 Both strategies present advantages and disadvantages. The first procedure is more open to
49 collaboration and incorporation of existing seismic hazard models developed at national or re-
50 gional scales.  does not inherently guarantee homogeneity, since the methodologies used to
51 construct each model are probably different, and the basic data sets are likely compiled follow-
52 ing different criteria and may exhibit different levels of completeness. The second approach
53 streamlines construction of a hazard input model with exclusive methodologies and data sets
54 and, therefore, presumably results in a more homogeneous model. Not only does the latter
55 approach diminish the role and contributions of the earthquake hazard community, however,
56 it may not even fully guarantee homogeneity since, firstly, data sets collected globally do not
57 necessarily guarantee a spatially constant quality and, secondly, the adequacy of a particular

58 modeling approach varies greatly depending on the available information and the tectonic con-
59 text.

60  December 2018, at the culmination of its second implementation phase (2015–2018),
61 GEM completed the first version of the global earthquake model, releasing a global seismic
62 hazard map (Pagani et al., 2018), as described herein, and a global exposure database and global
63 risk map described by Silva et al. (2019). Supplementing the hazard results obtained within
64 GEM’s second implementation phase, a global homogenized instrumental earthquake catalog
65 (Weatherill et al., 2016) and a Global Active Fault Database (Styron and Pagani, 2019) were
66 produced. The latter in particular expands on the work formerly done within the Faulted Earth
67 project (Christoffersen et al., 2015) and regional databases created in the framework of GEM
68 projects (e.g. South America, Caribbean and Central America). These products, along with
69 the results of the global projects completed by GEM during its first implementation phase from
70 2009 to 2014 (Pagani et al., 2015), were key for the development of hazard models in areas
71 where GEM was unable to form collaborations with local institutions.

72 In this paper, we describe the criteria used to compile the GEM hazard mosaic. We discuss
73 the main characteristics of the included models, and the procedure used to construct a global
74 homogenized map.  Finally, we compare properties of the computed hazard map to previously
75 released models.

76 THE CRITERIA USED TO COMPILE THE GEM MOSAIC

77 The mosaic is built upon the GEM principle of openness, and so the primary condition for
78 including a model is the ability for GEM to openly share it. Given the commitment to achieve
79 a first global coverage by the end of 2018, we compiled the GEM mosaic following selection
80 criteria with a balance between pragmatism and GEM’s principles of collaboration, openness,
81 and transparency. 

82 In order to efficiently achieve this goal, we selected a model for each region using a three-
83 tier approach. Tier 1 includes models developed by either an internationally recognized national
84 agency, or a cooperative scientific project involving several organizations. Models in this tier
85 generally rely on the broadest involvement of the local scientific community and incorporate
86 high scientific and technical standards; therefore, Tier 1 represents what we consider the ideal
87 case. The selected Tier 1 models include several national models, such as the 2014 USGS na-
88 tional seismic hazard model for Conterminous US (Petersen et al., 2014), the national seismic

89 hazard model for Japan (Headquarters for Earthquake Research Promotion (HERP), 2014), the
90 2015 version of the Canada National hazard model (Adams et al., 2015), the 2017 version of
91 the Indonesia national model (Irsyam et al., Submitted), and the 2018 version of the Australia
92 national model (Allen et al., Submitted). Many of the regional models are also Tier 1, includ-
93 ing the SHARE project in Europe (Woessner et al., 2015) and the EMME model in the Middle
94 East (Seşetyan et al., 2018), each created by an associated project, and the South America Risk
95 Assessment (SARA) project in South America (supported by the Swiss Re Foundation) and the
96 Caribbean and Central America Risk Analysis (CCARA) project in Central America and the
97 Caribbean (supported by the United States Agency for International Development (USAID),
98 which were constructed during GEM-promoted projects in collaboration with partner organiza-
99 tions.

100 In areas where Tier 1 models are not available, we applied the second selection criterion,
101 searching for models published in the literature (Tier 2) with sufficient detail to implement
102 into the OpenQuake-engine. Where this was not possible, GEM developed its own seismic
103 hazard models for the remaining uncovered areas (Tier 3), either by partnering with another
104 organization, or led solely by hazard modelers working within the GEM Secretariat.

105 The hazard inputs for all models included in the mosaic use the standard format of the
106 OpenQuake-engine (Pagani et al., 2014). This consists of at minimum three components: two
107 logic trees describing epistemic uncertainty in the seismic source characterization (SSC) and
108 in the ground motion characterization (GMC), and at least one seismic source model (SSM).
109 A SSM is a list of sources accounting for all possible seismicity of engineering importance in
110 the proximity of the investigated area; individual sources in the SSM only consider aleatory
111 uncertainty. The GMC consists of weighted ground motion models (GMMs) for each tectonic
112 region.

113 For the models included in the mosaic that were not originally implemented in the OpenQuake-
114 engine, we developed codes to automatically convert the original models to the OpenQuake-
115 engine format. Translating a hazard model from one software format to another often requires
116 modeling decisions that attempt to replicate implicit modeling decisions inherent to the original
117 software. This is possible because of the OpenQuake-engine's flexible framework. For exam-
118 ple, we followed this approach to incorporate various models produced by the United States
119 Geological Survey (USGS), as well as the national hazard model for Japan.

120 Having the whole suite of models represented with a common format offers several advan-

121 tages. Firstly, a global hazard map or similar product is more easily computed from a suite of
122 models that all comply with a standard format. Secondly, the common format offers simplified
123 utility to users of the hazard mosaic and use of the OpenQuake-engine format in particular en-
124 sures that the models can be easily used with the GEM-developed and maintained OpenQuake-
125 engine (Pagani et al., 2014). Future updates and additions to the global hazard mosaic will
126 continue to follow this formatting standard.

127 **THE COMPONENTS OF THE GEM MOSAIC AND THEIR GENERAL** 128 **CHARACTERISTICS**

129 The GEM Mosaic is a collection of 30 Probabilistic Seismic Hazard Analysis (PSHA) input
130 models designed to compute seismic hazard at large scales (Table 1 and Figure 1). Fourteen are
131 national or sub-national models, while the remaining are regional models. The oldest included
132 model is the USGS Hawaii model (Klein et al., 2001); all the other models were published after
133 2007. Overall, the GEM mosaic contains about 3.5 million earthquake sources that generate
134 around 1.8 billion ruptures. The GMC includes about 90 ground-motion prediction equations
135 subdivided into various tectonic regions (e.g. Active Shallow Crust, Stable Continental Crust).
136 Here, we describe each of the models included in the GEM Mosaic, covering the globe by
137 geographic region. Rather than providing a homogenous description of the various models, we
138 highlight the characteristics that make the respective model novel or unique, or that categorize
139 it methodologically (or otherwise) with some of the other included models.

140 **NORTH AMERICA**

141 Six models were used to compute hazard in North America. From north to south, these include:
142 the 2007 USGS Alaska model (Wesson et al., 2007, 2008); the 2015 Canada national hazard
143 model produced by Natural Resources Canada (Adams et al., 2015); the 2014 USGS National
144 Seismic Hazard Model (Petersen et al., 2014) in combination with version 3 of the Unified
145 California Earthquake Rupture Forecast (UCERF3, Field et al. (2014)); a seismic hazard model
146 for Mexico developed by GEM; and the regional hazard model covering Central America and
147 the Caribbean, prepared in the framework of the CCARA project.

148 The hazard input model for Alaska (Wesson et al., 2007, 2008) is based on the typical frame-
149 work used by the USGS for the construction of seismic hazard analyses, both within the United
150 States as well as for territories overseas. Shallow seismicity is accounted for by a combination

Table 1. Components of the GEM Mosaic

Acr.	Year	Region covered	Tier	Project	Reference publications
ALS	2007	Alaska	1		Wesson et al. (2007, 2008)
ARB	2018	Arabian Peninsula	1		Zahran et al. (2015, 2016)
AUS	2018	Australia	1		Allen et al. (Submitted)
CAN	2015	Canada	1		Adams et al. (2015)
CCA	2018	Caribbean, C. America	1	CCARA	
CEA	2018	Central Asia	1	EMCA	Ullah et al. (2015)
CHN	2015	China	1		Gao (2015)
EUR	2013	Europe	1	SHARE	Woessner et al. (2015)
HAW	1998	Hawaii	1		Klein et al. (2001)
IDN	2017	Indonesia	1		Irsyam et al. (Submitted)
IND	2012	India and surroundings	2		Nath and Thingbaijam (2012)
JPN	2014	Japan	1		HERP (2014)
KOR	2018	Korean Peninsula	3		Gao (2015), HERP (2014)
MEX	2018	Mexico	3		
MIE	2016	Middle-East	1	EMME	Danciu et al. (2017, 2018); Seşetyan et al. (2018)
NAF	2018	Northern Africa	3		Poggi et al. (2019)
NEA	2018	Northeastern Asia	3		
NWA	2018	Northwestern Asia	3		
NZL	2010	New Zealand	1		Stirling et al. (2012)
PHL	2018	Philippines	3		Penarubia et al. (Submitted)
PAC	2018	Pacific Islands	3		Johnson and Pagani (in prep.)
PNG	2015	Papua New Guinea	1		Ghasemi et al. (2016)
SAM	2018	South America	1	SARA	Garcia et al. (2017)
SEA	2018	Southeast Asia	1		Ornthammarath et al. (Submitted)
SSA	2018	Sub-Saharan Africa	1	SSAHARA	Poggi et al. (2017)
TEM	2015	Taiwan	1		Wang et al. (2016)
UCF	2014	California	1		Field et al. (2014)
USA	2014	Conterminous U.S.	1		Petersen et al. (2015)
WAF	2018	Western Africa	3		
ZAF	2018	South Africa	1		Midzi et al. (2019)

151 of smoothed seismicity and fault sources, while subduction earthquakes are separated into in-
152 terface earthquakes generated by fault sources with a 3D geometry, and intraslab earthquakes
153 organized as layers of point sources obtained by smoothing hypocentral depth-based classes of
154 intraslab seismicity.

155 The model for Canada is the 5th Generation national hazard model created by Natural Re-
156 sources Canada (Adams et al., 2015). Compared to the previous version, it contains several
157 improvements including, for the first time, a probabilistic computation of hazard generated by
158 the Cascadia subduction zone. The SSC is organized into four quadrants: two covering the
159 eastern and western Arctic regions, one comprising British Columbia and part of the West, and
160 one incorporating Ontario, Quebec, and Atlantic Canada. The 2015 Canada model is, to our
161 knowledge, the first national hazard model accounting for epistemic uncertainty in the ground
162 motion model via the backbone approach (Atkinson and Adams, 2013).

163 The 2014 USGS National Seismic Hazard Model for the Conterminous United States uti-
164 lized in the GEM mosaic includes two hazard models. The UCERF3 model (Field et al., 2014)
165 covers California, while a more conventional model is used to compute hazard for all the other
166 states (Petersen et al., 2014). Hazard calculation with these two models required the implemen-
167 tation of additional features in the OpenQuake-engine, including a specific calculator for the
168 UCERF3 model, and extended classical and event-based calculators that consider the cluster
169 model in the New Madrid Fault Zone (Petersen et al., 2008, 2014). The implementation of the
170 UCERF3 model was particularly challenging, as it required adding to the OpenQuake-engine
171 the ability to compute hazard from seismic source models with a peculiar structure (Field et al.,
172 2014). Specifically, these adaptations enabled the software to build the earthquake rupture fore-
173 cast directly from the input file, thus adding the ability to incorporate rupture configurations
174 that would not normally be supported by common parametric definitions of earthquake sources.

175 The model for Mexico was created by the GEM hazard team. The SSC includes 3D fault
176 sources modeling shallow seismicity and subduction interface earthquakes, point sources ac-
177 counting for shallow distributed seismicity in active and stable crust, and 3D ruptures con-
178 strained within the volume of the slab accounting for the deep subduction seismicity. The
179 crustal faults are modified from the catalog by Villegas et al. (2017). The GMC consists of sets
180 of GMMs for each of the four tectonic regions considered. The selection of GMMs was per-
181 formed using residual analysis of strong ground-motion data for a set of candidate GMMs. The
182 strong-motion data was provided by the National Autonomous University of Mexico (UNAM,

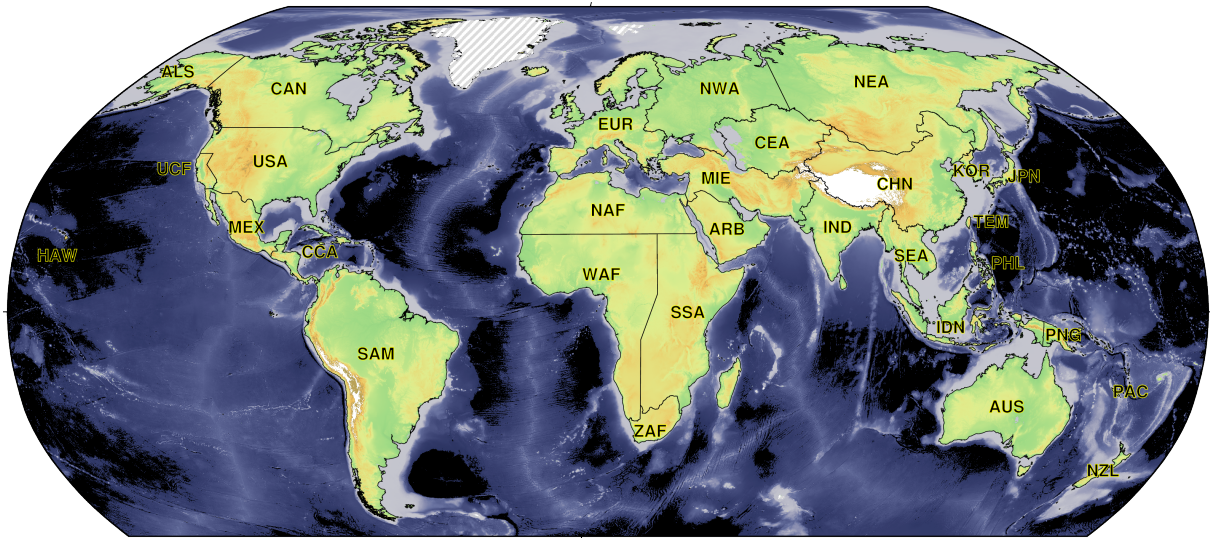


Figure 1. Geographic coverage of the models included in the GEM mosaic (version 2018.1).

183 <http://www.ssn.unam.mx/>) and the Center for Scientific Research and Higher Education at En-
 184 senada (CICESE, <http://resnom.cicese.mx/>).

185 The core of the model for the Caribbean and Central America was developed within the
 186 CCARA project, with additions that cover Cuba and Puerto Rico. The structure of the hazard
 187 input model resembles that of the Mexico model. It includes three major subduction zones: the
 188 Middle American subduction system, extending along the Pacific coast from Panama to south-
 189 ern Mexico, the eastern Caribbean (Lesser Antilles) subduction system and the Puerto Rico-
 190 Hispaniola subduction system, proximal to the northeastern corner of the Caribbean Plate. An
 191 active fault database (Styron et al., 2018a) was developed for the CCARA project, which was the first
 192 active fault dataset mapped by GEM for the GEM Global Active Faults database; this regional
 193 database served as the template for the global database (Styron et al., 2018a). As with the Mex-
 194 ico model, we completed the GMC via a residual analysis on a local strong-motion database
 195 containing recordings from both the Caribbean and Central America. Data from the Lesser An-
 196 tilles was retrieved from the Engineering Strong-Motion database (ESM, <https://esm.mi.ingv.it>),
 197 while the Ministerio de Medio Ambiente y Recursos Naturales (MARN, <http://m.marn.gob.sv/>)
 198 provided the recordings for El Salvador through a bilateral collaboration with GEM.

199 SOUTH AMERICA

200 In South America, the SSC consists of a single source model originally created for the SARA
 201 project (Garcia et al., 2017), and subsequently updated by the GEM hazard team. The structure

202 of the hazard input model resembles that of the Mexico and Caribbean and Central America
203 models. In most of this region, hazard is dominated by the subduction sources located along
204 the western coast of the continent. Local shallow faults control hazard peaks throughout the
205 Andean cordillera and foreland (?). The GMC (Drouet et al., 2017) contains a set of GMMs
206 for each tectonic region, selected using an extensive residual analysis performed on a database
207 of strong-motion recordings collected for several countries in the region, including Colombia,
208 Ecuador, Chile and Brazil. The pattern of hazard computed is generally consistent with the one
209 described by Petersen et al. (2018) with peaks of hazard concentrated in the central part of Chile
210 and in Ecuador.

211 **EUROPE AND AFRICA**

212 The SHARE model Woessner et al. (2015) was selected for calculating seismic hazard in Eu-
213 rope. The SHARE project - funded by the European Union under the Seventh Framework
214 Programme (FP7) was the first GEM regional project, and was a collaboration that paved the
215 way for the construction of similar models in other areas. This model was also an important
216 test case in the early development of the OpenQuake-engine, as it was used to challenge the
217 software capability to compute hazard at a continental scale. The SHARE SSC is composed of
218 three source models developed with different initial data sets and modeling strategies. The first
219 and most traditional model was obtained by harmonizing the geometries of area sources defined
220 in published national hazard models. The second model represented a novelty for Europe, as
221 it used fault sources extensively for hazard calculation, particularly in the active and extended
222 shallow crust regions (Delavaud et al., 2012). The third model was a smoothed seismicity model
223 obtained with the application of a new method proposed by Hiemer et al. (2014).

224 The model for Northern Africa (Poggi et al., 2019) was built by the GEM Hazard Team
225 using an earthquake catalog covering the entire region and new database of shallow active faults
226 (Styron and Poggi, 2019) compiled as part of the construction of GEM's Global Active Fault
227 database. The SSC consists of two source models: one which includes both smoothed seismicity
228 and fault sources with simple geometry, and a second containing only smoothed seismicity. In
229 the latter, epistemic uncertainty for the seismicity rates is considered.

230 The model covering the East African Rift system is the latest evolution of work origi-
231 nally performed within the GEM-AfricaArray collaboration in the context of the Sub-Saharan
232 Africa Hazard and Risk Assessment (SSAHARA, see Poggi et al. (2017)). The model includes

233 smoothed seismicity within source zones with geometries mostly aligned parallel to the Rift
234 Valley axis, starting from the Gulf of Aden until Zimbabwe where the rift splays into a number
235 of minor tectonic structures. The GMC is particularly uncertain in this region—and more gen-
236 erally in Africa—given the complete absence of strong-motion recordings. The GMC contains
237 a logic tree with five tectonic regions allowing a transition from pure active shallow crust to a
238 stable continental region through a weighted combination of models normally assigned to these
239 two classes.

240 The model for Western Africa covers an area entirely classified as stable crust (see, for
241 example, Chen et al. (2018)). It was developed by the GEM Hazard Team using primarily
242 information taken from literature (Poggi, 2019). One of the most prominent earthquake sources
243 in this model, located in Ghana, is probably related to fault structures within the Western African
244 Shield (Amponsah, 2004).

245 South Africa is covered by the model of Midzi et al. (2019), which was produced by a
246 collaboration between the Council of Geoscience in South Africa and the Indian Institute of
247 Technology. Because of the low level of seismicity and limited data, the SSC is inherently
248 uncertain, and so the authors incorporate alternative Gutenberg-Richter, maximum magnitude,
249 and depth values to account for epistemic uncertainty (discussed more in Section 4).

250 ASIA

251 Asia is the most complex continent in terms of both the number of hazard models included in the
252 GEM Mosaic as well as their seismotectonic diversity. We describe the main characteristics of
253 the thirteen models chosen, going from West to East. The westernmost coverage of Asia is the
254 Earthquake Model for the Middle East (EMME; (Seşetyan et al., 2018)), which extends from
255 the western coast of Turkey to Afghanistan and Pakistan. This model includes the Caucasian
256 countries (Georgia, Armenia and Azerbaijan), Iran, and countries in the Middle East bordering
257 the Mediterranean Sea. The EMME model was created by a large group of local scientists, and
258 represented an important achievement with respect to seismic hazard assessment in the region.
259 The project also facilitated the compilation of new basic data sets including an earthquake cat-
260 alogue (Zare et al., 2014), an active fault database (Danciu et al., 2017) and a strong-motion
261 database (Danciu et al., 2018). The EMME SSC contains two seismic source models (Danciu
262 et al., 2017). The first uses area sources to model active shallow crustal seismicity, shallow
263 stable crustal seismicity, and subduction intraslab seismicity in combination with fault sources

264 producing interface ruptures in the Makran subduction region. The second model accounts for
265 distributed seismicity using a grid of points with rates obtained from a seismicity smoothing
266 process.

267 The model for the Arabian Peninsula (Zahran et al., 2015, 2016) was developed by the Saudi
268 Geological Survey (SGS), and implemented into the OpenQuake-engine within a collaboration
269 between GEM and SGS. Volcanic activity in the proximity of the Red Sea poses particular
270 challenges to hazard modeling in this region, because it controls the location of some of the
271 earthquake sources as well as the attenuation of seismic waves within the crust 

272 The Earthquake Model for Central Asia (EMCA; Ullah et al. (2015)) covers Kyrgyzstan,
273 Tajikistan, Turkmenistan, Uzbekistan, and Kazakhstan. The model was developed within a
274 project lead by the GeoForschungsZentrum (GFZ) in Potsdam, Germany. The SSC consists
275 of a single seismic source model containing only area sources, while the GMC contains one
276 set of GMMs for active shallow crustal sources and one single GMM for stable continental
277 crust. As in various other areas, the paucity of strong-motion recordings leads to large epistemic
278 uncertainties that are not yet fully captured in the GMC component of the logic tree.

279 We compute hazard in the Northern part of Asia using two models that together cover the en-
280 tire Russian territory, split around the 76°E meridian. In the Northwestern Asia model (NWA),
281 seismicity mostly occurs within cratonic and stable crust, spanning an area of low seismic haz-
282 ard.  The Northeastern Asia model  (NEA) covers Mongolia and the eastern part of Russia. The
283 seismic source model contains a newly collected set of active faults in belts extending from
284 southwestern Mongolia north and east to the Arctic and Pacific coasts and islands (Styron et al.,
285 2018b) 

286 We implemented the most recent national seismic hazard model for China (Gao, 2015)
287 through a collaboration with the Institute of Geophysics of the China Earthquake Administra-
288 tion. The SSC for this model comprises area sources that are hierarchically organized using
289 three levels of delineation, where each level includes a further subdivision and a larger number
290 of sources. The GMC contains four GMMs: one per tectonic region covered by this model.

291 For Taiwan, we used the most recent model version produced by the Taiwan Earthquake
292 Model (Wang et al., 2016), one of the public organizations supporting GEM. The SSC for
293 this hazard model contains a single seismic source model, based on area sources to model
294 shallow distributed seismicity, and faults with simple geometry to model large earthquakes in
295 the shallow crust, on the subduction interface, and within the subducting slab.

296 For Japan, GEM collaborated with the National Research Institute for Earth Science and
297 Disaster Resilience (NIED) to translate the 2014 version of the model developed by the Head-
298 quarters for Earthquake Research Promotion (HERP) into the OpenQuake-engine format. This
299 model is unique in that the SSC includes mutually exclusive ruptures on some subduction
300 interface faults, an aspect that required the addition of some computational features to the
301 OpenQuake-engine. For example, the largest interface earthquakes in the Nankai subduction
302 are modeled using this approach which in the investigation timeframe (i.e. 30 or 50 years)
303 admits only the occurrence of a large event. The GMC uses a single GMM for each tectonic
304 region.

305 Although no national model for the Korean Peninsula was available, coverage was obtained
306 by merging sources from both the China and Japan national model. The model is a combination
307 of area sources from the China national model, which model shallow seismicity, and subduction
308 sources from the Japan national model. For the GMC, we used primarily the recommendations
309 of Stewart et al. (2013).

310 The seismic hazard model for India and the surroundings, including Nepal and Bangladesh,
311 was developed by Nath and Thingbaijam. The SSC for this model accounts for epistemic un-
312 certainty in an unequally weighted logic tree of three seismic source models: one comprising of
313 area sources, and two using smoothed seismicity but adopting different minimum magnitudes.
314 The GMC uses a set of GMMs for each modeled tectonic region, and further divides active
315 shallow crust into two categories based on faulting mechanism. This model was implemented
316 in the OpenQuake-engine by N. Ackerley (Natural Resources Canada).

317 For Southeast Asia, the Earth Observatory of Singapore and Mahidol University devel-
318 oped two seismic source models, which are combined to create the SSC for this region (Orn-
319 thamarath et al., Submitted). The two source models were developed independently and are
320 weighted equally in the logic tree. A single GMC is used for both seismic source models, which
321 uses a set of GMMs for each of the three tectonic region types within the GEM Mosaic coverage
322 by this model (active shallow crust, subduction interface, and subduction intraslab).

323 The Philippines is covered by a national PSHA model developed in the by a scientific collab-
324 oration between GEM and the Philippine Institute of Volcanology and Seismology (PHIVOLCS)
325 (Penarubia et al., Submitted), which aimed to expand upon previous work done by PHIVOLCS.
326 The SSC follows the approach used for the South America, Caribbean and Central America,
327 and Mexico models. The seismic source model includes a fault database derived from the

328 PHIVOLCS compilation used in 2017, but with updated fault characteristics. The GMC uses a
329 set of GMMs for each tectonic region, where the crustal GMM set is based partly on residual
330 analysis.

331 The GEM mosaic coverage of Indonesia uses the most recent national seismic hazard model,
332 developed by a pool of local organizations in collaboration with Geoscience Australia (Irsyam
333 et al., Submitted). Overall, the SSC structure follows the one used by the USGS for the develop-
334 ment of the most recent hazard models for the United States and territories. Because this work
335 built upon many years of collaboration with the USGS (e.g. Petersen et al., 2004), the model
336 was partly implemented in OpenQuake-engine, but also partly in the USGS NSHMP software,
337 and subsequently translated into the OpenQuake-engine format.

338 **OCEANIA**

339 Oceania is covered by the national seismic hazard models for Australia, New Zealand, and
340 Papua New Guinea, a regional model for the Pacific Islands, and the Hawaii sub-national model.

341 The Australia model was released in 2018 (Allen et al., Submitted) and represents the latest
342 model produced by Geoscience Australia. The SSC includes a logic tree with twenty indepen-
343 dently developed seismic source models based on diverse modeling assumptions, all of which
344 have national coverage, are either peer-reviewed or submitted to conference proceedings, and
345 are open access. The source models were assigned unequal weights during compilation of the
346 final SSC.

347 The New Zealand seismic hazard model is an updated version of the 2010 national seismic
348 hazard model published by Stirling et al., the outcome of an effort involving a pool of organi-
349 zations led by GNS Science. The SSC includes distributed seismicity and faults sources mod-
350 eled as planar surfaces with characteristic recurrence rates. Sources follow a Poisson model of
351 earthquake occurrence, with the exception of four fault sources with time-dependent recurrence
352 intervals. The GMC uses a single GMM for each tectonic region.

353 For Papua New Guinea, we adopted the seismic hazard model proposed by Ghasemi et al.
354 (2016). This model was developed within a collaboration between Geoscience Australia and the
355 Geophysical Observatory in Port Moresby. The SSC uses two branches: one consisting solely
356 of smoothed seismicity, and a second that combines complex faults and area sources. The GMC
357 is based partly on residual analysis performed in an earlier study by Petersen et al. (2012).

358 Because seismic source modeling is particularly challenging in Hawaii, where most seis-
359 micity is controlled by volcanism, few recent studies have modeled the seismic hazard of the
360 Hawaiian Island. We chose to include the model of Klein et al. (2001) in the GEM Mosaic.
361 The SSC includes a number of formerly activated faults with complex geometry along vol-
362 canic flanks on Hawaii Island, and both area and smoothed seismicity sources capturing the
363 distributed seismicity. GMC is also complicated for this island chain, given the peculiar atten-
364 uation characteristics in the volcanic area and the limited number of strong-motion recordings
365 available.

366 Finally, the hazard model for the Pacific Islands (Johnson and Pagani, in prep.) was devel-
367 oped by the GEM Hazard Team following a scheme similar to that described for the models of
368 Mexico, the Caribbean and Central America, South America, and the Philippines. The model
369 adopts the GMC used for neighboring Papua New Guinea.

370 **A SUMMARY OF THE MAIN CHARACTERISTICS OF MODELS IN THE GEM** 371 **MOSAIC**

372 Overall, the described set of PSHA models provides a comprehensive summary of probabilistic
373 seismic hazard analyses at the national and regional scales performed across the world. Here,
374 we present a short summary of key properties, starting with a general discussion on epistemic
375 uncertainty.

376 The input format for the OpenQuake-engine contains two logic tree structures accounting
377 for epistemic uncertainty in the SSC and GMC, respectively. Remarkably, out of a total of 30
378 models, only four of them do not consider epistemic uncertainty in the GMC logic tree. GMC
379 uncertainty is taken into account by defining a set of GMMs for each tectonic region considered
380 in the logic tree. The only exception to this standard approach is the ground motion logic tree
381 used in the 2015 version of the Canada national hazard model, which captures uncertainty using
382 a backbone approach with high, low, and mid estimates (Atkinson and Adams, 2013; Atkinson
383 et al., 2014).

384 In the collection of included models, the use of epistemic uncertainty in the SSC is more
385 variable. Thirteen models incorporate this type of uncertainty, mainly by defining alternative
386 seismic source models that capture the variability in the geometry and location of earthquake
387 sources and their occurrence properties. The SSC logic tree with the largest number of seismic
388 source models is the latest national hazard model for Australia (Allen et al., Submitted), which

389 contains 18 different source models. The South Africa model (Midzi et al., 2019) is an example
390 from this model suite that uses an alternative means of capturing source model uncertainty, as
391 in this case the logic tree contains epistemic uncertainties on Gutenberg-Richter parameters and
392 maximum magnitude for each individual source out of the 22 area sources considered. Other
393 models with articulated logic tree structures (e.g. Adams et al., 2015) were also implemented in
394 the OpenQuake-engine and included in the mosaic, but with their SSMs in a collapsed form in
395 order to reduce calculation complexity.

396 With respect to the typologies of sources used in the various models, the widespread use of
397 shallow fault sources in active and stable shallow crust is notable; twenty models include this
398 source typology. Most of the models without fault sources are located in stable areas where
399 identifying active structures is in general more challenging. Overall (but excluding sources in
400 the UCERF3 model) the GEM mosaic contains more than 25,000 fault sources of simple and
401 characteristic typologies, using the OpenQuake-engine terminology 

402 In the subduction areas, common practice in the GEM Mosaic suite of models is to separate
403 the sources accounting for subduction interface versus intraslab seismicity. Interface sources,
404 given their variability in geometry, are modeled using complex fault geometries (Pagani et al.,
405 2014). On the contrary, the modeling of intraslab sources is more variable. Some models
406 (e.g. Indonesia National Hazard Model, US National Hazard Model) contain point sources
407 obtained by smoothing seismicity within various hypocentral depth intervals, some model intraslab
408 seismicity using faults (e.g. Taiwan model), some use area sources with different hypocentral
409 depths, and some model intraslab seismicity with a set of finite ruptures constrained within the
410 slab volume.

411 GLOBAL HAZARD MAPS

412 The global hazard map released at the end of 2018 (see Figure 2) displays seismic hazard in
413 terms of the geographic distribution of the peak ground acceleration (PGA) with 10% proba-
414 bility of being exceeded (PoE) in 50 years for a reference site condition characterized by an
415 average shear wave velocity in the range 760-800 m/s in the uppermost 30 meters, a range
416 which represents rock conditions according to commonly used site classification schemes  The
417 areas exhibiting the highest levels of seismic hazard are the coasts of the Pacific Ocean, the
418 Himalayan thrusts, Indonesia, Turkey and California. Overall, the Alpine-Himalayan chain is
419 the widest contiguous area exhibiting moderate to high values of seismic hazard 

420 Since the GEM mosaic contains a variety of models created using different approaches and
421 methodologies, the hazard results at the border between models will inevitably show discordant
422 values. In order to minimize these discontinuities in the pattern of hazard, and to obtain a
423 gradual transition of the iso-probable values of shaking between models, we developed an ad-
424 hoc methodology to harmonize the hazard results across models.

425 HOMOGENIZATION OF HAZARD CURVES

426 The methodology adopted for combining the hazard computed with the models in the GEM
427 mosaic relies on a reference global grid of points used to calculate results. The geometry of
428 this grid can have different characteristics; we chose a grid that is (almost) equally spaced in
429 distance. Every model has a corresponding computation area (Figure 1) used to extract a subset
430 of points - which we call ,“sites” - from the global grid. We use a buffer of about 75 km around
431 each computation area in order to have a sufficiently large band of overlapping sites across each
432 border between adjacent models.

433 Notably, from a purely scientific perspective, the hazard map obtained through this homog-
434 enization procedure might obscure potential hazard differences at the borders between models.
435 Scientists interested in studying those differences are invited to use results directly obtained
436 for individual models using the OpenQuake-engine. The methodology described herein—with
437 minor modifications—can be used to thoroughly study these differences.

438 In order to obtain global homogenized hazard maps, we sequentially analyze every model
439 and store the corresponding hazard curve for each site in either a final repository if the site is
440 inside the model, or in temporary repository if the site is within one of the buffer regions. In a
441 second phase, we further process the hazard curves for sites located within the buffer between
442 models. In most of the cases, sites within a buffer region have two hazard curves, one for each
443 model across which the buffer is placed. For a minor number of sites concentrated in Asia, there
444 are more than two hazard curves assigned. This occurs, for example, near the contact between
445 the models of China, Central Asia, the Middle East, and India.

446 The homogenization of hazard curves is completed by processing each point included in the
447 temporary repository. For each site, we compute the shortest distance to the border between
448 models, d_b , and use this distance to compute a weight for each hazard curve. For hazard curves
449 at sites occupying the computation area of the model, we assign an initial weight equal to the
450 sum of the buffer distance and d_b . On the contrary, for the hazard curves of sites within the

451 buffer region but outside the computation area of the model, the initial weight is equal to the
452 difference between the buffer distance and d_b . Weights are subsequently normalized by their
453 sum, used to compute the contribution of each hazard curve, and collocated curves are summed
454 to yield the final homogenized curve. For a given site, each ordinate of the hazard curve is
455 obtained as follows:

$$poe_{iml} = poe_{iml}^{inside} * w^{inside} + poe_{iml}^{outside} * w^{outside} \quad (1)$$

456 COMPARISONS WITH PREVIOUS DATA AND MODELS

457 Over the last 20 years, the hazard map produced by the GSHAP project (Giardini et al., 1999)
458 represented a benchmark for depicting probabilistic seismic hazard at a global scale. In this
459 section, we illustrate similarities and fundamental differences between the GSHAP map and the
460 GEM map presented herein. Both the maps display PGA with 10% Probability of Exceedance
461 (PoE) in 50 years.

462 We discuss this appraisal using the maps in Figure 3. Each map contains areas filled with
463 three colors which indicate the following: Given a reference ground-motion threshold (gm_T),
464 for example 0.1 g, the green-filled areas show where both the GSHAP map and the GEM map
465 contain values of ground motion larger than gm_T , the blue-filled areas show the domains where
466 only the GSHAP model exceeds gm_T and, the red-filled areas show the regions where only the
467 GEM map has values of hazard higher than the threshold ground-motion gm_T .

468 Figure 3A shows the map obtained for a gm_T equal to 0.1g. Overall, the two maps exhibit
469 compatible results. The most striking differences appear in Australia, Northeastern Canada,
470 and the Caucasus, where the GSHAP map shows higher values of hazard; and India and the
471 Southern part of the East African Rift, where the hazard included in the GEM model shows
472 higher values.

473 In Figure 3B, the gm_T is increased to 0.3 g, and the differences between hazard pattern in
474 the two maps become more evident. In Asia, with the exception of India and South Pakistan, the
475 GSHAP model shows generally higher values of hazard compared to the ones in the GEM map.
476 The GEM map, on the contrary, indicates more prominent hazard than GSHAP in South Amer-
477 ica along the Andean Cordillera, in Central America, in Papua-New Guinea, and Indonesia. On
478 a coarser scale, we note that the GEM map tends to concentrate high hazard areas along major
479 subduction regions, whereas the GSHAP model puts more hazard along the Alpine-Himalayan
480 orogenic belt.

481 The trend just described is substantiated by the map in Figure 3C, computed for a gm_T of
482 0.5 g. In this plot the congruity of the two maps reduces even further and, as a consequence,
483 the green filled areas almost completely disappear. Red-filled areas confine to the proximity of
484 subduction regions, including the Himalayan thrusts, with the exception of Mexico, where the
485 two maps both exceed the gm_T of 0.5g. The blue-filled zones are mostly concentrated in Asia
486 (China, Hindu Kush and Kamchatka) 

487 CONCLUSIONS

488 The GEM hazard map and the GEM mosaic—the underlying database of hazard input models—
489 are the result of a major collective effort, which saw the contribution of dozens of organizations
490 and individuals. Because of this, the GEM mosaic is a comprehensive summary of the most re-
491 cent publicly accessible hazard input models developed at national and regional scale produced
492 globally over the last ten years.

493 The GEM global hazard map released at the end of 2018 constitutes an update of hazard
494 computed at the global scale using a collection of hazard models, as originally done within the
495 GSHAP project (Giardini et al., 1999). The GSHAP and GEM hazard maps show similar pat-
496 terns of hazard when we consider the exceedance of moderate levels of hazard for a reference
497 return period of 475 years, while the two maps exhibit more dissimilarity in geographic distri-
498 butions considering the areas affected by the highest levels of hazard. The GEM map identifies
499 the areas located in the proximity of the most important subduction sources as the most dan-
500 gerous ones, whereas the GSHAP map highlights sections of the Alpine-Himalayan orogenic
501 belt.

502 We hope that the GEM mosaic will promote a collaborative, bottom-up approach to the con-
503 struction of more homogenous seismic hazard models, notwithstanding the difficulty of prop-
504 erly defining what exactly represents a set of homogenous hazard models. In our opinion, the
505 degree of homogeneity between the SSC in two different hazard input models must be analyzed
506 by taking into account the adopted methodologies, the information used, and the tectonic con-
507 text covered. The latter is important since the methods used to build models often depend on the
508 tectonic region in question. Differences between SSCs can also be assessed during a-posteriori
509 tests of the models, for example through comparisons between the predicted earthquake occur-
510 rences and the observations collected after the release of the model. The homogeneity between
511 distinct GMCs is easier to compare, as it depends on the GMMs selected per tectonic region

512 and their similarity. In the coming years, GEM plans to explore ways to compare hazard models
513 with the aim to promote discussion and development of more homogeneous and conceptually
514 compatible seismic hazard models. This will start with the creation of a more comprehensive set
515 of tools for comparing various characteristics between models (see, for example, (Pagani et al.,
516 2016) and between hazard models and basic information used for their construction, such as
517 earthquake catalogs, fault databases, tectonic and geodetic information, and strong-motion data.

518 As a database, the GEM mosaic offers a number of scientific opportunities, and renders
519 hazard information for some parts of the globe that was previously unavailable. Its accessibility
520 to the scientific community gives it the potential to serve as a modern benchmark for newly
521 developed models, which might later be incorporated into the collection. Notably, components
522 of the mosaic fill knowledge gaps in regions that were previously only partially covered by
523 updated models, such as in some parts of Africa. More generally, the GEM mosaic has the
524 potential to promote innovations and a more thorough understanding of our current state of
525 knowledge, starting from the most important and challenging issues that will be faced when new
526 models are constructed in the various tectonic regions. Additional research could be developed
527 on top of the mosaic models, such as the study of secondary hazards, the incorporation of
528 aftershock contribution into regular hazard analyses, and infrastructure risk.

529 The GEM Mosaic is built upon a dynamic framework, in which the database of models
530 will be maintained to include the most up-to-date openly available hazard information. This
531 framework includes the OpenQuake-engine, the open source tools developed by GEM and part-
532 ner organizations for the construction of hazard input model components, and the collection of
533 hazard models described in this paper. In the future, GEM aims to incorporate updates of exist-
534 ing models and to expand the number of national hazard models included in the mosaic. Both
535 these efforts will be carried out, to the extent possible, with the largest participation of experts
536 from various regions of the world. The map will be updated using current versions of the GEM
537 mosaic on an approximately yearly basis.

538 **References**

- 539 Adams, J., Halchuk, S., Allen, T., and Rogers, G., 2015. Canada's 5th Generation Seismic Hazard
540 Model, as Prepared for the 2015 National Building Code of Canada. In *Proceedings of the 11th*
541 *Canadian Conference on Earthquake Engineering*.
- 542 Allen, T. I., Griffin, J., Leonard, M., Clark, D., and Ghasemi, H., Submitted. The 2018 National Seismic
543 Hazard Assessment of Australia: Quantifying Hazard Changes And Model Uncertainties. *Earthquake*
544 *Spectra* .

- 545 Amponsah, P. E., 2004. Seismic activity in Ghana: past, present and future. *Annals of Geophysics* **47**.
546 doi:10.4401/ag-3319.
- 547 Atkinson, G. M. and Adams, J., 2013. Ground motion prediction equations for application to the 2015
548 Canadian national seismic hazard maps. *Canadian Journal of Civil Engineering* **40**, 988–998. doi:
549 https://doi.org/10.1139/cjce-2012-0544.
- 550 Atkinson, G. M., Bommer, J. J., and Abrahamson, N. A., 2014. Alternative Approaches to Modeling
551 Epistemic Uncertainty in Ground Motions in Probabilistic Seismic-Hazard Analysis. *Seismological*
552 *Research Letters* **85**, 1141–1144. doi:10.1785/0220140120.
- 553 Chen, Y.-S., Weatherill, G., Pagani, M., and Cotton, F., 2018. A transparent and data-driven global
554 tectonic regionalization model for seismic hazard assessment. *Geophysical Journal International*
555 **213**, 1263–1280. doi:10.1093/gji/ggy005.
- 556 Christophersen, A., Litchfield, N., Berryman, K., Thomas, R., Basili, R., Wallace, L., Ries, W., Hayes,
557 G. P., Haller, K. M., Yoshioka, T., Koehler, R. D., Clark, D., Wolfson-Schwehr, M., Boettcher, M. S.,
558 Villamor, P., Horspool, N., Ornthammarath, T., Zuñiga, R., Langridge, R. M., Stirling, M. W., Goded,
559 T., Costa, C., and Yeats, R., 2015. Development of the Global Earthquake Model's neotectonic fault
560 database. *Natural Hazards* **79**, 111–135. doi:10.1007/s11069-015-1831-6.
- 561 Danciu, L., Kale, O., and Akkar, S., 2018. The 2014 Earthquake Model of the Middle East: ground
562 motion model and uncertainties. *Bulletin of Earthquake Engineering* pp. 1–37. doi:10.1007/s10518-
563 016-9989-1.
- 564 Danciu, L., Şeşetyan, K., Demircioglu, M., Gülen, L., Zare, M., Basili, R., Elias, A., Adamia, S.,
565 Tsereteli, N., Yalçın, H., Utkucu, M., Khan, M. A., Sayab, M., Hessami, K., Rovida, A. N., Stuc-
566 chi, M., Burg, J.-P., Karakhanian, A., Babayan, H., Avanesyan, M., Mammadli, T., Al-Qaryouti, M.,
567 Kalafat, D., Varazanashvili, O., Erdik, M., and Giardini, D., 2017. The 2014 Earthquake Model
568 of the Middle East: seismogenic sources. *Bulletin of Earthquake Engineering* pp. 1–32. doi:
569 10.1007/s10518-017-0096-8.
- 570 Delavaud, E., Cotton, F., Akkar, S., Scherbaum, F., Danciu, L., Beauval, C., Drouet, S., Douglas, J.,
571 Basili, R., Sandikkaya, M. A., Segou, M., Faccioli, E., and Theodoulidis, N., 2012. Toward a ground-
572 motion logic tree for probabilistic seismic hazard assessment in Europe. *Journal of Seismology* **16**,
573 451–473. doi:10.1007/s10950-012-9281-z.
- 574 Dimaté, C., Drake, L., Yopez, H., Ocola, L., Rendon, H., Grünthal, G., and Giardini, D., 1999. Seis-
575 mic hazard assessment in the Northern Andes (PILOTO Project). *Annals of Geophysics* **42**. doi:
576 10.4401/ag-3787.
- 577 Drouet, S., Montalva, G., Dimaté, M. C., Castillo, L. F., and Fernandez, G. A., 2017. Building a Ground-
578 Motion Logic Tree for South America within the GEM-SARA Project Framework. In *Proceedings of*
579 *the 16th World Conference on Earthquake Engineering*.
- 580 Field, E. H., Arrowsmith, R. J., Biasi, G. P., Bird, P., Dawson, T. E., Felzer, K. R., Jackson, D. D.,
581 Johnson, K. M., Jordan, T. H., Madden, C., Michael, A. J., Milner, K. R., Page, M. T., Parsons, T.,
582 Powers, P. M., Shaw, B. E., Thatcher, W. R., Weldon, R. J., and Zeng, Y., 2014. Uniform California
583 Earthquake Rupture Forecast, Version 3 (UCERF3)—The Time-Independent Model. *Bulletin of the*
584 *Seismological Society of America* **104**, 1122–1180. doi:10.1785/0120130164.
- 585 Gao, M., 2015. *Publicizing Textbook of China Seismic Hazard Map*. China Standard Press (in Chinese).
- 586 Garcia, J., Weatherill, G. W., Pagani, M., Rodriguez, L., Poggi, V., and the SARA Working Group,
587 2017. Building an Open Seismic Hazard Model for South America: the SARA-PSHA Model. In
588 *Proceedings of the 16th World Conference on Earthquake Engineering*.
- 589 Ghasemi, H., McKee, C., Leonard, M., Cummins, P., Moihoi, M., Spiro, S., Taranu, F., and Buri, E.,

590 2016. Probabilistic seismic hazard map of Papua New Guinea. *Natural Hazards* **81**, 1003–1025.
591 doi:10.1007/s11069-015-2117-8.

592 Giardini, D., Grünthal, G., Shedlock, K. M., and Zhang, P., 1999. The GSHAP global seismic hazard
593 map. *Annali di Geofisica* **42**, 1225–1230.

594 Headquarters for Earthquake Research Promotion (HERP), 2014. *The National Seismic Hazard Map*
595 *2014 Version—With an Overview on the Ground Motion Hazard of the Whole Country*. Tech. rep.,
596 Headquarters for Earthquake Research Promotion. (in Japanese).

597 HERP, 2014. *The National Seismic Hazard Map 2014 Version—With an Overview on the Ground Motion*
598 *Hazard of the Whole Country*. Tech. rep., Headquarters for Earthquake Research Promotion. (in
599 Japanese).

600 Hiemer, S., Woessner, J., Basili, R., Danciu, L., Giardini, D., and Wiemer, S., 2014. A smoothed stochas-
601 tic earthquake rate model considering seismicity and fault moment release for Europe. *Geophysical*
602 *Journal International* **198**, 1159–1172. doi:10.1093/gji/ggu186.

603 Irsyam, M., Cummins, P., Faisal, L., Natawidjaja, D. H., Widiyantoro, S., Meilano, I., Triyoso, W.,
604 Rudiyanto, A., Hidayati, S., Ridwan, M., and Hanifa, R., Submitted. Development of the 2017
605 National Seismic Hazard Maps of Indonesia. *Earthquake Spectra* .

606 Johnson, K. and Pagani, M., in prep. Seismic Hazard Model For the Pacific Islands. *In preparation* .

607 Klein, F. W., Frankel, A. D., Mueller, C. S., Wesson, R. L., and Okubo, P. G., 2001. Seismic Hazard
608 in Hawaii: High Rate of Large Earthquakes and Probabilistic Ground-Motion Maps. *Bulletin of the*
609 *Seismological Society of America* **91**, 479–498. doi:10.1785/0120000060.

610 Midzi, V., Manzunzu, B., Mulabisana, T., Zulu, B. S., Pule, T., Myendeki, S., and Rathod, G. W., 2019.
611 The Probabilistic Seismic Hazard Assessment of South Africa. *Journal of Seismology* .

612 Nath, S. K. and Thingbaijam, K. K. S., 2012. Probabilistic Seismic Hazard Assessment of India. *Seis-*
613 *mological Research Letters* **83**, 135–149. doi:10.1785/gssrl.83.1.135.

614 Ordaz, M. G., Cardona, O.-D., Salgado-Gálvez, M. A., Bernal-Granados, G. A., Singh, S. K., and
615 Zuloaga-Romero, D., 2014. Probabilistic seismic hazard assessment at global level. *International*
616 *Journal of Disaster Risk Reduction* **10**, 419–427. doi:10.1016/j.ijdrr.2014.05.004.

617 Ornthammarath, T., Warnitchai, P., Chan, C.-H., Wang, Y., Shi, X., Nguyen, P. H., Nguyen, J. M.,
618 Kosuwan, S., Thant, M., and Sieh, K., Submitted. Probabilistic Seismic Hazard Assessments for
619 Northern Southeast Asia (Indochina): Smooth Seismicity Approach. *Earthquake Spectra* .

620 Pagani, M., Garcia, J., Monelli, D., Weatherill, G., and Smolka, A., 2015. A summary of hazard datasets
621 and guidelines supported by the Global Earthquake Model during the first implementation phase.
622 *Annals of Geophysics* **58**. doi:10.4401/ag-6677.

623 Pagani, M., Garcia-Pelaez, J., Gee, R., Johnson, K., Poggi, V., Styron, R., Weatherill, G., Simionato, M.,
624 Viganò, D., Danciu, L., and Monelli, D., 2018. Global Earthquake Model (GEM) Seismic Hazard
625 Map (version 2018.1 - December 2018). doi:10.13117/GEM-GLOBAL-SEISMIC-HAZARD-MAP-
626 2018.

627 Pagani, M., Hao, K. X., Fujiwara, H., Gerstenberger, M., and Ma, K.-F., 2016. Appraising the PSHA
628 Earthquake Source Models of Japan, New Zealand, and Taiwan. *Seismological Research Letters* **87**,
629 1240–1253. doi:10.1785/0220160101.

630 Pagani, M., Monelli, D., Weatherill, G., Danciu, L., Crowley, H., Silva, V., Henshaw, P., Butler, L.,
631 Nastasi, M., Panzeri, L., Simionato, M., and Viganò, D., 2014. OpenQuake Engine: An Open Hazard
632 (and Risk) Software for the Global Earthquake Model. *Seismological Research Letters* **85**, 692–702.
633 doi:10.1785/0220130087.

- 634 Penarubia, H., Johnson, K. L., Styron, R. H., Bacolcol, T. C., Bonita, J. D., Narag, I. C., Perez, J. S.,
635 Sevilla, W. I. G., Solidum Jr., R. G., Pagani, M., and Allen, T. I., Submitted. Probabilistic Seismic
636 Hazard Analysis model for the Philippines. *Earthquake Spectra* .
- 637 Petersen, M., Moschetti, M., Powers, P., Mueller, C., Haller, K. M., Frankel, A., Zeng, Y., Rezaeian, S.,
638 Harmsen, S., Boyd, O., Field, E., Chen, R., Rukstales, K., Luco, N., Wheeler, R., Williams, R., and
639 Olsen, A., 2014. *Documentation for the 2014 update of the United States national seismic hazard
640 maps. Open-File Report 2014–1091*, U.S. Geological Survey.
- 641 Petersen, M. D., Dewey, J., Hartzell, S., Mueller, C., Harmsen, S., Frankel, A., and Rukstales, K.,
642 2004. Probabilistic seismic hazard analysis for Sumatra, Indonesia and across the Southern Malaysian
643 Peninsula. *Tectonophysics* **390**, 141–158. doi:10.1016/j.tecto.2004.03.026.
- 644 Petersen, M. D., Frankel, A. D., Harmsen, S. C., Mueller, C. S., Haller, K. M., Wheeler, R. L., Wesson,
645 R. L., Zeng, Y., Boyd, O. S., Perkins, D. M. et al., 2008. *Documentation for the 2008 update of the
646 United States national seismic hazard maps. Tech. rep.*, Geological Survey (US).
- 647 Petersen, M. D., Harmsen, S. C., Rukstales, K. S., Mueller, C. S., McNamara, D. E., Luco, N., and
648 Walling, M., 2012. *Seismic Hazard of American Samoa and Neighboring South Pacific Islands—
649 methods, Data, Parameters, and Results*. US Department of the Interior, US Geological Survey.
- 650 Petersen, M. D., Moschetti, M. P., Powers, P. M., Mueller, C. S., Haller, K. M., Frankel, A. D., Zeng,
651 Y., Rezaeian, S., Harmsen, S. C., Boyd, O. S. et al., 2015. The 2014 United States national seismic
652 hazard model. *Earthquake Spectra* **31**, S1–S30.
- 653 Petersen, M. D., Mueller, C. S., Moschetti, M. P., Hoover, S. M., Rukstales, K. S., McNamara, D. E.,
654 Williams, R. A., Shumway, A. M., Powers, P. M., Earle, P. S. et al., 2018. 2018 One-Year Seismic
655 Hazard Forecast for the Central and Eastern United States from Induced and Natural Earthquakes.
656 *Seismological Research Letters* **89**, 1049–1061.
- 657 Poggi, V., 2019. Seismic Hazard Model For Western Africa. *In preparation* .
- 658 Poggi, V., Durrheim, R., Tuluka, G. M., Weatherill, G., Gee, R., Pagani, M., Nyblade, A., and Delvaux,
659 D., 2017. Assessing seismic hazard of the East African Rift: a pilot study from GEM and AfricaArray.
660 *Bulletin of Earthquake Engineering* pp. 1–31. doi:10.1007/s10518-017-0152-4.
- 661 Poggi, V., Styron, R., and Garcia-Pelaez, J., 2019. Seismic Hazard Model For Northern Africa. *In
662 preparation* .
- 663 Seşetyan, K., Danciu, L., Demircioğlu Tümsa, M. B., Giardini, D., Erdik, M., Akkar, S., Gülen, L.,
664 Zare, M., Adamia, S., Ansari, A., Arakelyan, A., Askan, A., Avanesyan, M., Babayan, H., Chelidze,
665 T., Durgaryan, R., Elias, A., Hamzehloo, H., Hessami, K., Kalafat, D., Kale, O., Karakhanyan, A.,
666 Khan, M. A., Mammadli, T., Al-Qaryouti, M., Sayab, M., Tsereteli, N., Utkucu, M., Varazanashvili,
667 O., Waseem, M., Yağın, H., and Yılmaz, M. T., 2018. The 2014 seismic hazard model of the Middle
668 East: overview and results. *Bulletin of Earthquake Engineering* **16**, 3535–3566. doi:10.1007/s10518-
669 018-0346-4.
- 670 Silva, V., Amo-Oduro, D., Calderon, A., Costa, C., Dabbeek, J., Despotaki, V., Martins, L., Pagani,
671 M., Rao, A., Simionato, M., Viganò, D., Yepes-Strada, C., Acevedo, A., Crowley, H., Horspool, N.,
672 Jaiswal, K., Journey, M., and Pittore, M., 2019. Development of a Global Seismic Risk Model.
673 *Earthquake Spectra* .
- 674 Stewart, J. P., Douglas, J., Javanbarg, M., Bozorgnia, Y., Abrahamson, N. A., Boore, D. M., Camp-
675 bell, K. W., Delavaud, E., Erdik, M., and Stafford, P. J., 2013. Selection of Ground Motion
676 Prediction Equations for the Global Earthquake Model. *Earthquake Spectra* **31**, 19–45. doi:
677 10.1193/013013EQS017M.
- 678 Stirling, M., McVerry, G., Gerstenberger, M., Litchfield, N., Dissen, R. V., Berryman, K., Barnes,

- 679 P., Wallace, L., Villamor, P., Langridge, R., Lamarche, G., Nodder, S., Reyners, M., Bradley, B.,
680 Rhoades, D., Smith, W., Nicol, A., Petteinga, J., Clark, K., and Jacobs, K., 2012. National Seismic
681 Hazard Model for New Zealand: 2010 Update. *Bulletin of the Seismological Society of America* **102**,
682 1514–1542. doi:10.1785/0120110170.
- 683 Styron, R., Garcia-Pelaez, J., and Pagani, M., . CCAF-DB: The Caribbean and Central American Active
684 Fault Database. *Natural Hazards and Earth System Science* Submitted.
- 685 Styron, R., García-Pelaez, J., and Pagani, M., 2018a. GEM Central America and Caribbean Active
686 Faults Database. doi:10.13117/CENTRAL-AMERICA-CARIBBEAN-ACTIVE-FAULTS.
- 687 Styron, R. and Pagani, M., 2019. The GEM Global Active Faults Database (GAF-DB). *Earthquake
688 Spectra* .
- 689 Styron, R. and Poggi, V., 2018. GEM North Africa Active Fault Database. doi:10.13117/N-AFRICA-
690 ACTIVE-FAULTS.
- 691 Styron, R., Poggi, V., and Lunina, O. V., 2018b. GEM Northeastern Asia Active Fault Database. doi:
692 10.13117/NE-ASIA-ACTIVE-FAULTS.
- 693 Ullah, S., Bindi, D., Pilz, M., Danciu, L., Weatherill, G., Zuccolo, E., Ischuk, A., Mikhailova, N. N.,
694 Abdrakhmatov, K., and Parolai, S., 2015. Probabilistic seismic hazard assessment for Central Asia.
695 *Annals of Geophysics* **58**. doi:10.4401/ag-6687.
- 696 Villegas, G. C., Mendoza, C., and Ferrari, L., 2017. Mexico Quaternary Fault Database. *Terra Digitalis*
697 **1**, 1–9. doi:10.22201/igg.terradigitalis.2017.1.3.50.
- 698 Wang, Y.-J., Chan, C.-H., Lee, Y.-T., Ma, K.-F., Shyu, J. B. H., Rau, R.-J., Cheng, C.-T. et al., 2016.
699 Probabilistic seismic hazard assessments for Taiwan. *Terr. Atmos. Ocean. Sci.* **27**, 325–340.
- 700 Weatherill, G. A. and Pagani, M., 2014. From Smoothed Seismicity Forecasts to Probabilistic Seismic
701 hazard: Insights and Challenges from a Global Perspective. In *Proceedings of the Second European
702 Conference on Earthquake Engineering and Seismology*, p. paper n. 1026. Istanbul.
- 703 Weatherill, G. A., Pagani, M., and Garcia, J., 2016. Exploring earthquake databases for the creation of
704 magnitude-homogeneous catalogues: tools for application on a regional and global scale. *Geophysical
705 Journal International* **206**, 1652–1676. doi:10.1093/gji/ggw232.
- 706 Wesson, R. L., Boyd, O. S., Mueller, C. S., Bufe, C. G., Frankel, A. D., and Petersen, M. D., 2007.
707 *Revision of time-independent probabilistic seismic hazard maps for Alaska. Tech. rep.*, Geological
708 Survey (US).
- 709 Wesson, R. L., Boyd, O. S., Mueller, C. S., and Frankel, A. D., 2008. Challenges in making a seismic
710 hazard map for Alaska and the Aleutians. *Active Tectonics and Seismic Potential of Alaska Geophys-
711 ical Monograph Series* **179**, 385–397.
- 712 Woessner, J., Laurentiu, D., Giardini, D., Crowley, H., Cotton, F., Grünthal, G., Valensise, G., Arvidsson,
713 R., Basili, R., Demircioglu, M. B. et al., 2015. The 2013 European seismic hazard model: key
714 components and results. *Bulletin of Earthquake Engineering* **13**, 3553–3596.
- 715 Zahran, H. M., Sokolov, V., Roobol, M. J., Stewart, I. C., Youssef, S. E.-H., and El-Hadidy, M., 2016.
716 On the development of a seismic source zonation model for seismic hazard assessment in western
717 Saudi Arabia. *Journal of Seismology* **20**, 747–769.
- 718 Zahran, H. M., Sokolov, V., Youssef, S. E.-H., and Alraddadi, W. W., 2015. Preliminary probabilistic
719 seismic hazard assessment for the Kingdom of Saudi Arabia based on combined areal source model:
720 Monte Carlo approach and sensitivity analyses. *Soil Dynamics and Earthquake Engineering* **77**, 453–
721 468.
- 722 Zare, M., Amini, H., Yazdi, P., Sesetyan, K., Demircioglu, M. B., Kalafat, D., Erdik, M., Giardini, D.,

723 Khan, M. A., and Tsereteli, N., 2014. Recent developments of the Middle East catalog. *Journal of*
724 *Seismology* **18**, 749–772. doi:10.1007/s10950-014-9444-1.

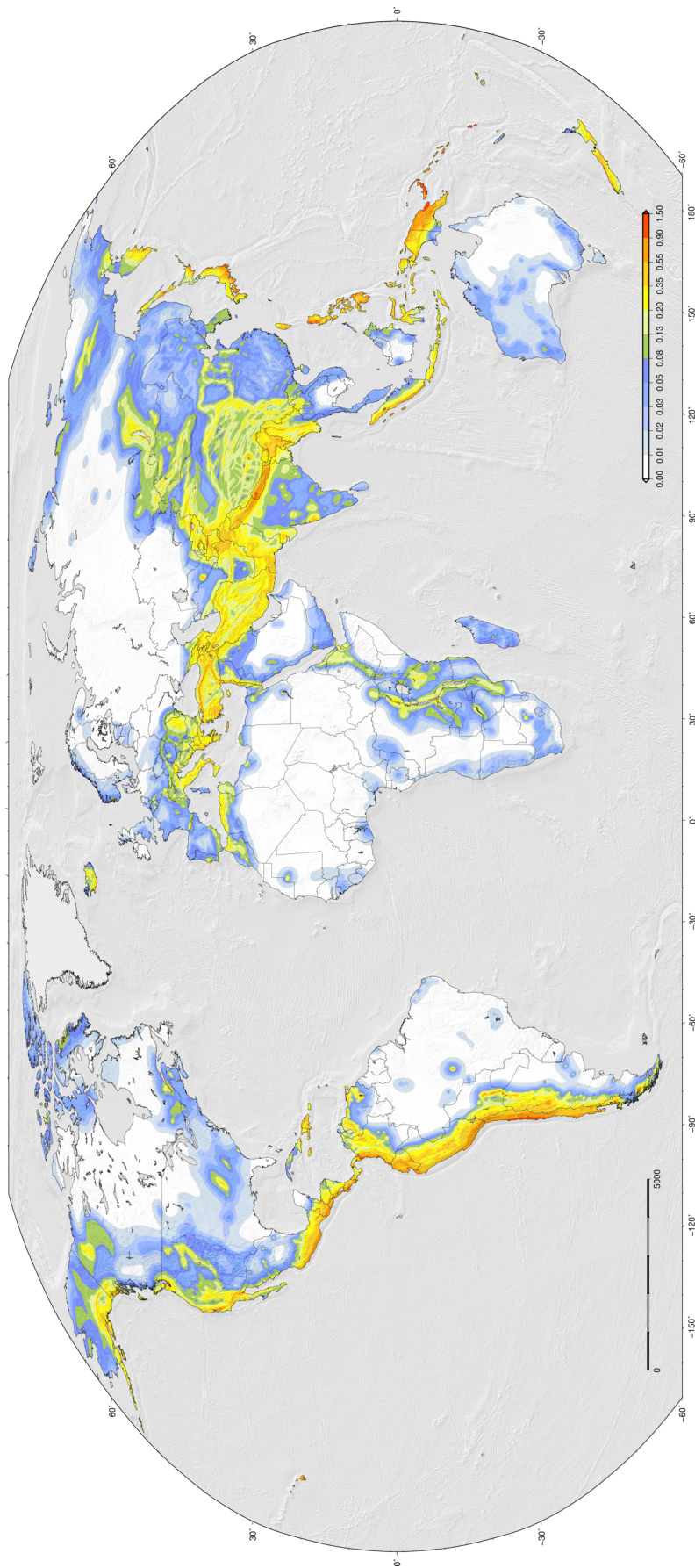


Figure 2. The GEM global hazard map (version 2018.1). The map displays Peak Ground Acceleration (PGA) with a 10% probability of being in exceeded in 50 years on reference soil conditions ($V_{s30}=760\text{-}800\text{m/s}$).

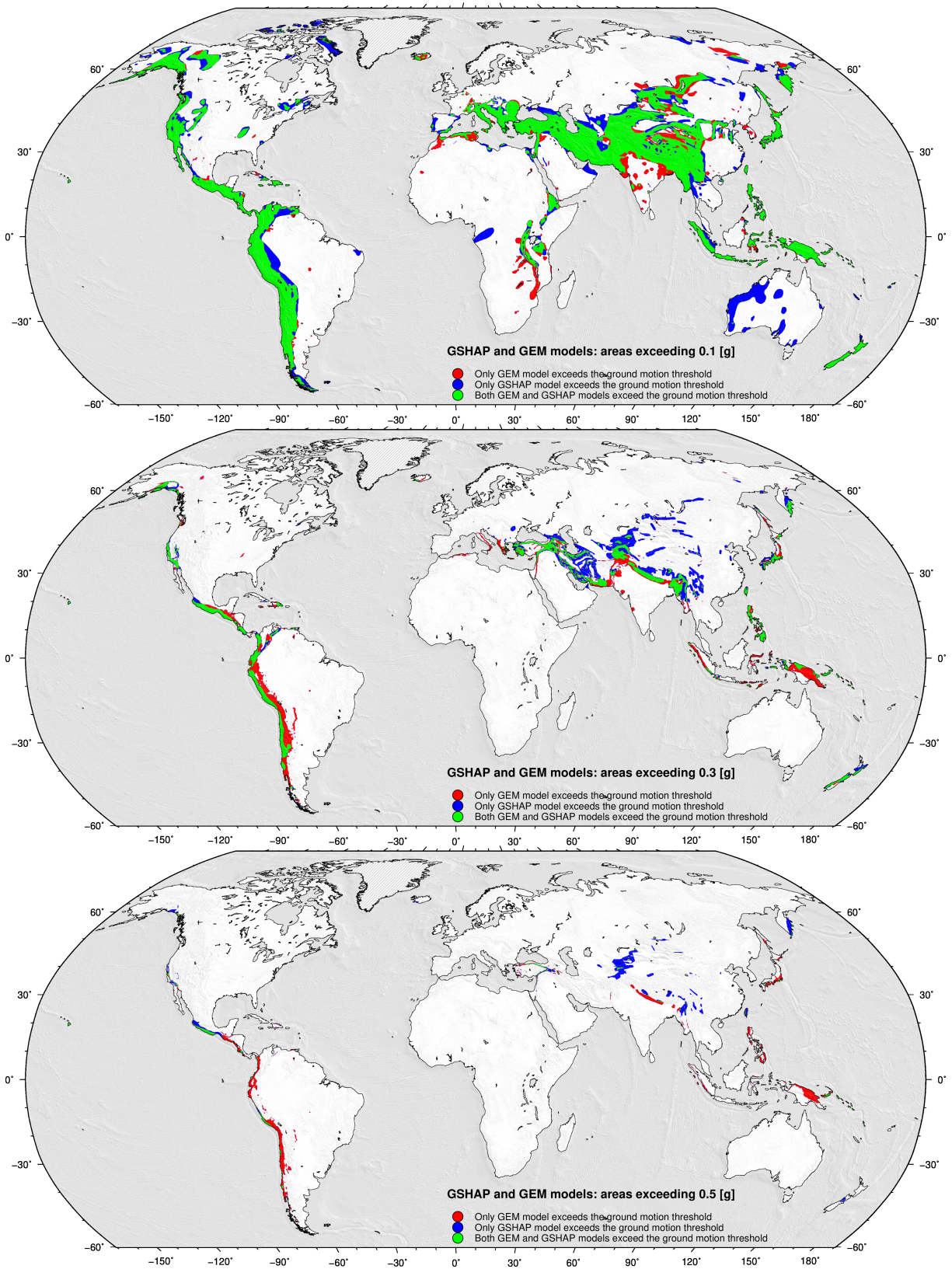


Figure 3. Maps comparing the pattern of hazard included in the GSHAP and GEM (version 2018.1) global hazard maps.